Ultraviolet Resonance Raman Spectra of Trp-182 and Trp-189 in Bacteriorhodopsin: Novel Information on the Structure of Trp-182 and Its Steric Interaction with Retinal

Shinji Hashimoto,[‡] Kohki Obata,[‡] Hideo Takeuchi,*[,‡] Richard Needleman,[§] and Janos K. Lanyi[||]

Pharmaceutical Institute, Tohoku University, Aobayama, Sendai 980-77, Japan, Department of Biochemistry, Wayne State University School of Medicine, Detroit, Michigan 48201, and Department of Physiology and Biophysics, University of California, Irvine, California 92697

Received June 11, 1997; Revised Manuscript Received July 18, 1997[⊗]

ABSTRACT: Ultraviolet (244 nm) resonance Raman spectra of Trp-182 and Trp-189 in bacteriorhodopsin were obtained by subtracting the spectrum of the mutants, Trp-182→Phe or Trp-189→Phe, from that of the wild-type. Analysis of the spectra shows that the $\chi^{2,1}$ torsion angle about the $C_\beta-C_3$ bond is ±93° for Trp-182 and ±100° for Trp-189. Both Trp residues are moderately hydrogen bonded to proton acceptors at their indolyl nitrogens in hydrophobic environments. The environmental hydrophobicity is particularly strong for Trp-182, as judged from the splitting of the W7 Raman band to a triplet. The Raman information on the structure and environment of Trp-189 is consistent with the molecular model from electron diffraction [Grigorieff et al. (1996) *J. Mol. Biol. 259*, 393−421]. On the other hand, the $\chi^{2,1}$ angle and the hydrogen-bonding state of Trp-182 found here differ from those in the model structure. Revision of the model to correspond to the Raman findings would require a 60° rotation of the Trp-182 indole ring about the $C_\beta-C_3$ bond toward the chromophore retinal and the presence of a water molecule that is hydrogen bonded to the indolyl nitrogen. The triplet feature of the W7 band of Trp-182 is attributable to unusually strong steric repulsion between the indole ring and the 9- and 13-methyl groups of the retinal. Resonance Raman spectra in the visible suggest that this steric conflict destabilizes the 13-*cis* isomeric state of the retinal.

Bacteriorhodopsin (bR[1]), a 26 kDa protein found in the purple membrane of *Halobacterium salinarium*, functions as a light-driven proton pump. The chromophore retinal of bR is attached to the protein through a protonated Schiff base (PSB) linkage to the ϵ-amino group of Lys-216. Isomerization of the retinal from *all-trans* to 13-*cis* upon light absorption triggers a cyclic photochemical reaction that involves a series of intermediates, bR → K ↔ L ↔ M ↔ N ↔ O → bR, each of which is characterized by a distinct absorption spectrum in the visible. During the photocycle, a proton is translocated from the cytoplasmic to the extracellular side, and the photon energy is converted into a transmembrane electrochemical potential. The proton translocation involves protonation and deprotonation of ionizable residues of the protein as well as of the Schiff base, while the isomerization of retinal may be associated with conformational changes of the protein (for recent reviews, see refs 1−5).

The polyene chain and the β-ionone ring of retinal are surrounded by hydrophobic residues that include four Trp residues at positions 86, 138, 182, and 189 (*6*, *7*). Time-resolved fluorescence studies had suggested the involvement of at least some (but unidentified) Trp residues in the photocycle (*8*, *9*). Indeed, UV−visible absorption studies demonstrated that replacement of Trp-86, Trp-182, or Trp-189 by Phe affected the optical properties of the intermediates and the kinetics of the photocycle (*10*−*12*). Structural information on individual Trp residues has been obtained by Fourier transform infrared (FTIR) spectroscopy, in combination with site-directed mutagenesis. Rothschild and co-workers found a frequency shift of the hydrogen out-of-plane (HOOP) vibration of the indole ring of Trp-86 in the K intermediate and ascribed the shift from the unphotolyzed state to perturbation by the retinal isomerization (*13*, *14*). Recently, Maeda et al. reported that the L intermediate is characterized by a prominent infrared band at 3486 cm^{-1}, assigned to the indole N−H stretching vibration of Trp-182, and concluded that the indole ring of Trp-182 is not hydrogen bonded in the L state (*15*, *16*). The 3486 cm^{-1} band disappeared in a bR analogue which contained 9-desmethylretinal (*16*), suggesting that interaction between the indole ring of Trp-182 and the 9-methyl group of retinal is responsible for the non-hydrogen-bonded state of Trp-182 in the L intermediate. Weidlich et al. have compared the effects of the Trp-182→Phe mutation with those of 9-demethylation of retinal on the UV−visible and FTIR spectra (*17*). The two modifications are found to affect the later part of the photocycle in similar manners, and these workers proposed that the interaction between Trp-182 and the 9-methyl group facilitates the 13-*cis* → *all-trans* reisomerization of the retinal and the proton uptake at the cytoplasmic surface (*17*).

Each of the Trp residues in the retinal-binding pocket may be expected to play its own role in the photocycle of bR,

[‡] Tohoku University.
[§] Wayne State University School of Medicine.
[||] University of California.
[⊗] Abstract published in *Advance ACS Abstracts,* September 1, 1997.
[1] Abbreviations: bR, bacteriorhodopsin; FTIR, Fourier transform infrared; FWHM, full-width at half-maximum; HEPES, *N*-2-hydroxymethylpiperazine-*N*′-2-ethanesulfonic acid; HOOP, hydrogen out-of-plane; λ_{max}, wavelength of absorption maximum; PSB, protonated Schiff base; UVRR, ultraviolet resonance Raman; VISRR, visible resonance Raman; WT, wild-type; W182F and W189F, bacteriorhodopsin mutants Trp-182→Phe and Trp-189→Phe.

S0006-2960(97)01404-9 CCC: $14.00

through interactions with the retinal and other amino acid residues in its vicinity. Revealing the structures and interactions of the individual Trp residues will contribute to understanding the role of these residues in the proton pump. Ultraviolet resonance Raman (UVRR) spectroscopy is a useful method to investigate structures and environments of aromatic amino acid side chains in proteins (*18*, *19*). Previous UVRR studies provided some pieces of information on the conformations, hydrogen-bonding states, and environmental hydrophobicity of Trp residues in bR (*20*−*26*). However, the interpretation of the UVRR spectra suffered from limitations because bR contains eight Trp residues in its 248-amino acid polypeptide chain (*27*), and each Trp Raman band was a superposition of Raman bands from all eight Trp residues. To obtain structural information on individual Trp residues, it is required to remove or shift Raman signals of particular Trp residues by biochemical modification or isotopic labeling. Point mutation is an effective method to remove the signals of a particular residue from the spectrum, as has been demonstrated by FTIR difference spectroscopy (reviewed in refs 1 and 5).

In this study, we focused on Trp-182 and Trp-189, which are, respectively, closest to the methyl groups and the ionone ring of the retinal chromophore (*6*, *7*). By using the mutants Trp-182→Phe (W182F) and Trp-189→Phe (W189F), we extracted the UVRR spectra of Trp-182 and Trp-189 from the UVRR spectrum of wild-type (WT) bR. This is possible because if the excitation wavelength for Raman scattering is appropriately selected, the Raman intensity of Phe is substantially weaker than that of Trp. We found that the UVRR spectrum for Trp-189 is generally consistent with the conformation, hydrogen-bonding state, and environmental hydrophobicity predicted by the molecular model for bR proposed from electron diffraction (*6*, *7*). In contrast, from the UVRR spectrum of Trp-182 we obtained unexpected information on the conformation and hydrogen-bonding state of this residue that is not in accord with the predictions. Another novel finding is that the W7 Raman band of Trp-182, which is sensitive to environmental hydrophobicity, shows up as a triplet. This unusual splitting of the W7 band is interpreted as due to abnormally strong steric interaction of Trp-182 with the 9- and 13-methyl groups of the retinal.

EXPERIMENTAL PROCEDURES

Preparation of Samples. The *bop* gene containing either the W182F or the W189F residue replacement was expressed in *Halobacterium salinarium* L33 strain, as described previously (*28*), and the cells were cultured according to the procedure of Needleman et al. (*29*). Purple membranes of wild-type (WT) and mutant bR were purified by the standard method (*30*) and stored at −35 °C in 40% (w/w) sucrose. Sucrose was washed out just prior to spectrometric measurements by centrifugation in 5 mM *N*-2-hydroxyethylpiperadine-*N*′-2-ethanesulfonic acid (HEPES) buffer (pH 7.4). The buffer contained 100 mM Na_2SO_4, which was used as an internal intensity standard in UVRR measurements. The salt had no effect on the absorption spectra. All the chemicals used were of the highest grade and not further purified.

Dark and Light Adaptation. Dark adaptation of bR was made by keeping the sample in the dark at 4 °C for at least 48 h prior to spectroscopic analysis. Light adaptation was performed in a cuvette of 1 mm path length by exposing the bR membrane suspension to orange light emitted from a 300 W slide projector and filtered with a color filter (Toshiba, O-53). Although prolonged exposure did not change the visible absorption spectrum of WT bR, the mutant protein was gradually bleached by the irradiation. Accordingly, the exposure period was kept to a minimum (30 s) for the mutants. The bleaching was less than 1%.

Determination of Extinction Coefficients for Mutants. Bleached membranes were prepared by the hydroxylamine treatment described by Oesterhelt et al. (*31*), followed by dialysis against 5 mM HEPES buffer (pH 7.4) to remove hydroxylamine. Reconstitution of purple membranes was carried out according to a standard method (*32*). Microliter quantities of *all-trans* retinal dissolved in ethanol were added to 2 mL of the bleached bR suspension in the dark and absorption spectra were recorded after the equilibrium was reached (∼40 min). The concentration of retinal in the ethanol solution was determined using an extinction coefficient of 42 800 M^{-1} cm^{-1} at 382 nm (*32*). The extinction coefficients of the mutants were determined at the isosbestic point of dark-light adaptation from the slope of absorbance increase (after dilution correction) against the amount of added retinal. The titration experiment was repeated at least four times to ensure reproducibility. Absorption spectra were recorded on a diode-array spectrophotometer (Beckman, DU-7500) with an accumulation time of 2.5 s.

Resonance Raman Measurement. The concentration of bR for Raman measurements was determined by using the absorbance at the isosbestic point of dark-light adaptation. The contribution of light scattering by the membrane fragments was removed from the absorption spectrum by assuming the following equation:

$$A = a\lambda^b \tag{1}$$

where A is the apparent absorbance due to light scattering and λ is the wavelength. The parameters a and b were adjusted to reproduce the baseline curve.

UVRR spectra of aromatic amino acid residues were excited with the 244 nm continuous wave radiation (power, 3 mW; beam diameter, 200 μm at the sample) from an intracavity frequency-doubled Ar ion laser (Coherent, Innova 300 FReD). About 5 mL of dark-adapted bR in 5 mM HEPES buffer (pH 7.4, containing 100 mM Na_2SO_4) was recirculated through a rectangular quartz cell by using a peristaltic pump. The scattered light was collected with a 90° scattering geometry and focused onto the entrance slit of a UV Raman spectrometer (*33*) equipped with a CCD detector (Princeton Instrument, UV-enhanced LN/CCD1152). Since we noticed that the self-absorption effect was a serious problem in the 90° scattering geometry, the concentration of bR was kept constant at 100 μM and the distance from the center of the laser beam to the inner wall of the quartz cell (self-absorption path length) was carefully adjusted to 150 μm with a micrometer stage on which the quartz cell was mounted. The spectrometer was calibrated by using Raman bands of a cyclohexanone-acetonitrile mixture (1:1, v/v) and the peak frequencies of sharp Raman bands were reproducible to within ±1 cm^{-1}. During the Raman measurements, the reservoir of the bR suspension was immersed in an ice bath to minimize sample heating. Absorption spectra of bR were recorded before and after the Raman measurement to check possible damages by the laser irradia-

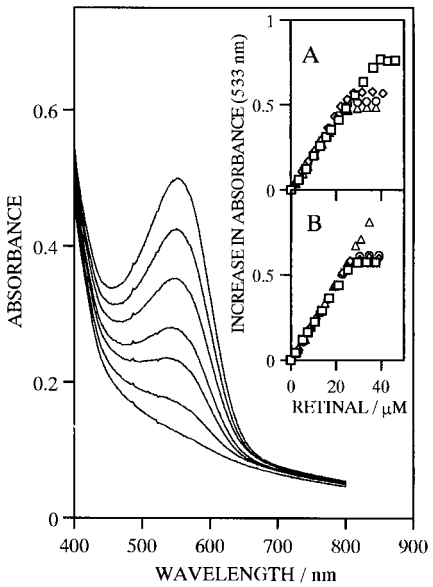

FIGURE 1: Absorbance changes during the titration of bleached membrane of W182F with *all-trans* retinal. Each spectrum was recorded after 40 min incubation at room temperature in order to achieve equilibrium. The inset shows absorbance increases of (A) W182F and (B) W189F against the concentration of added retinal. The slope of absorbance increase gives the extinction coefficient. Different symbols stand for different sets of titration.

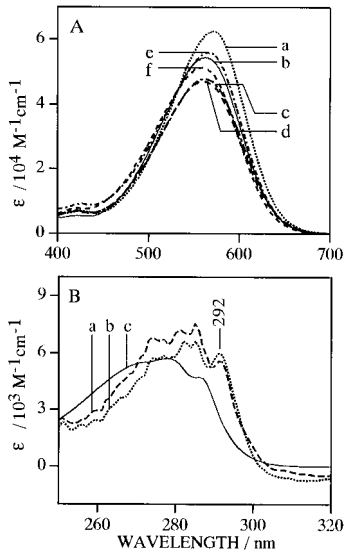

FIGURE 2: Absorption spectra of WT bR, W182F, and W189F in 5 mM HEPES buffer (pH 7.4). (Panel A) Visible absorption spectra of (a) WT bR, (c) W182F, and (e) W189F in the light-adapted state and (b) WT bR, (d) W182F, and (f) W189F in the dark-adapted state. Path length, 1 mm; accumulation time, 2.5 s; light scattering due to the membrane fragments is subtracted. (Panel B) Difference spectra of (a) WT bR − W182F and (b) WT bR − W189F and (c) the spectrum of aqueous Trp in the UV region.

tion. The decrease of the visible absorption intensity was less than 5% after 1 h exposure to the UV laser beam.

Raman spectra of the retinal chromophore were excited with the 514.5 nm line (2 mW) from an Ar ion laser (Coherent, Innova 70). About 3 mL of light-adapted bR suspension in HEPES buffer (pH 7.4; bR concentration, ~100 μM) was recirculated through a capillary cell (inner diameter, 0.5 mm) at a flow rate of 8.5 mL/min by using a peristaltic pump. The laser beam was focused onto the capillary cell (beam diameter, ~50 μm) and the Raman scattered light was collected in a 180° backscattering geometry. A Raman spectrometer (JASCO, NR1800) equipped with a CCD detector (Princeton Instrument, LN/CCD512) was used to record the spectrum. The spectrometer was calibrated with indene Raman bands and the peak frequencies of sharp Raman bands were accurate to ±0.5 cm^{-1}. Under the circulation conditions described above, bR molecules passed through the laser beam in 70 μs at a speed of 72 cm s^{-1} and only early photointermediates were expected to reside in the laser focus in addition to unphotolyzed bR (*1*−*5*). Of the early photointermediates, the K intermediate has a very short lifetime and the M intermediate is not resonant with the 514.5 nm excitation; thus, both were undetectable in the Raman spectrum. The 514.5 nm excited Raman spectrum showed a weak shoulder at 1551 cm^{-1}, which might be assigned to one of the strongest Raman bands of the L intermediate (*34*). However, the intensity of the shoulder was negligible. The N intermediate of W182F mutant has an unusually long lifetime of several seconds (*17*), but the contribution from the long-lived N intermediate was also negligible because bR molecules were exposed to the probe beam at intervals of 20 s.

RESULTS

Extinction Coefficients of the Mutants. Figure 1 shows absorption spectra for the titration of bleached W182F. Addition of retinal to a suspension of bleached bR regenerates the purple chromophore, and the absorbance in the visible region increases with the concentration of added retinal. The absorbance increase will be linear as long as all retinal added binds to bleached bR, and in that case the extinction coefficient of the purple pigment can be obtained from the slope of the absorbance increase (*32*). The inset to Figure 1 shows the absorbance increase at the isosbestic point of dark-light adaptation (533 nm for both W182F and W189F) as a function of retinal concentration (panel A, W182F; panel B, W189F). The absorbance increase is linear at retinal concentrations below 20−40 μM. The extinction coefficient determined from the slope of absorbance increase is 40 300 ± 1000 M^{-1} cm^{-1} for W182F and 44 900 ± 900 M^{-1} cm^{-1} for W189F. Similar titration of bleached WT bR gave an extinction coefficient of 45 100 ± 700 M^{-1} cm^{-1} at its isosbestic point (533 nm). This corresponds to an extinction coefficient of 63 000 ± 1000 M^{-1} cm^{-1} at the wavelength of the absorption maximum (λ_{max}, 568 nm) for light-adapted WT bR. The value agrees with the previously reported one (*32*).

UV−*Visible Absorption Spectra.* Figure 2A shows the absorption spectrum of WT bR, W182F, and W189F, in both dark- and light-adapted states. Light adaptation causes an intensity increase and a red shift of the absorption band of WT bR (compare traces a and b). The retinal chromophore is in the *all-trans* configuration in light-adapted WT bR, but assumes a 6:4 mixture of 13-*cis* and *all-trans* isomers in the dark-adapted state (*35*). The difference in isomeric ratio is mainly responsible for the spectral changes. Similar but smaller spectral changes are also observed for W189F (e, f), suggesting significant but smaller changes of the retinal isomeric population upon light adaptation. In contrast, the absorption spectrum of W182F is little affected by illumination (c,d). This implies that the retinal isomeric ratio in W182F might not be affected by the light adaptation. The unusually low extinction coefficient of this mutant in both

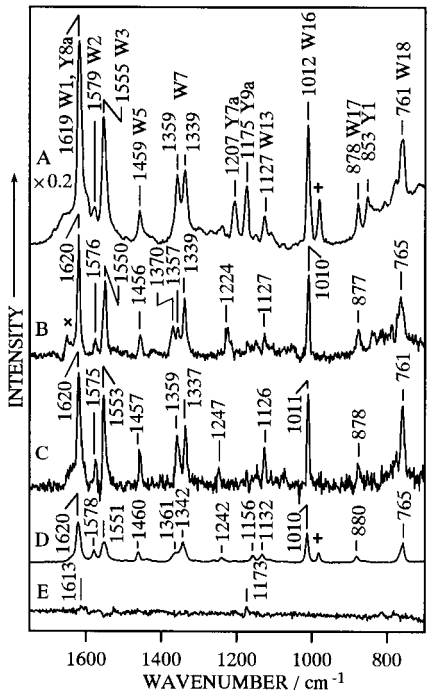

FIGURE 3: UVRR (244 nm) spectra of bR. (A) Dark-adapted WT bR (100 μM) in 5 mM HEPES buffer (pH 7.4) containing 100 mM Na_2SO_4. The Trp and Tyr bands are labeled with the mode notations of Harada and Takeuchi (*18*). (B) Difference spectrum WT bR − W182F showing the contribution of Trp-182 to spectrum A. ×, C═C stretch band of unsaturated lipid in the purple membrane (the unsaturated lipid content depends on the culture conditions). (C) Difference spectrum WT bR − W189F showing the contribution of Trp-189 to spectrum A. (D) aqueous Trp. (E) Difference spectrum between the light- and dark-adapted states of WT bR. The intensity of each spectrum was scaled using the SO_4^{2-} band at 982 cm^{-1} marked with +.

dark- and light-adapted states may partly be ascribed to a high content of the 13-*cis* isomer. Another possible factor that might reduce the extinction coefficient is a change in electronic properties of the retinal environment associated with the replacement of Trp-182 by Phe.

Figure 2B shows the absorption difference spectra, WT bR − W182F (a) and WT bR − W189F (b), in the UV region, together with the absorption spectrum of Trp in aqueous solution (c). Since the absorption of Phe is very weak in this spectral region, the absorption in each difference spectrum is ascribed to the L_a (∼270 nm) and L_b (∼290 nm) transitions of the Trp residue that is mutated to Phe. In contrast to the structureless band shape of aqueous Trp (c), the L_b absorption bands of Trp-182 and Trp-189 show well-resolved vibrational structures, suggesting that these side chains are buried in hydrophobic environments (*36*). For 3-methyl indole (a model compound for Trp), the λ_{max} of the 0-0 transition of the L_b absorption band is shifted from 290 to 292 nm when the indole ring is hydrogen bonded to a proton acceptor in a hydrophobic solvent (data not shown). The 0-0 transitions for both Trp-182 and Trp-189 are at 292 nm, suggesting that the indolyl nitrogens of these Trp residues are likewise hydrogen bonded in hydrophobic environments.

UVRR Spectra of Trp-182 and Trp-189. The 244 nm excited UVRR spectrum of dark-adapted WT bR is shown in Figure 3A. WT bR contains 32 aromatic (8 Trp, 11 Tyr, and 13 Phe) residues (*27*), which absorb UV light in the 200−300 nm region. With 244 nm excitation, however, the scattering from Phe is considerably weaker than from Trp and Tyr, and the prominent Raman bands in the spectrum are assignable to the 8 Trp and the 11 Tyr residues, as indicated with labels W and Y, respectively. The predominance of Trp Raman scattering over the Phe scattering may be exploited in obtaining the UVRR spectra of particular Trp residues in WT bR by using Trp→Phe mutants. If the mutation of a Trp residue to Phe does not affect the Raman bands of the other Trp and Tyr residues, the mutation simply removes the contribution from the Trp residue to the UVRR scattering, and the spectrum of that Trp residue can be obtained by subtracting the spectrum of the mutant from that of WT bR.

The UVRR spectrum for Trp-182 obtained by such spectral subtraction, *i.e.*, WT bR − W182F (both in the dark-adapted state), is shown in Figure 3B. The Raman bands of Tyr at 1207 (Y7a) and 1175 cm^{-1} (Y9a) are almost canceled out in the difference spectrum, indicating that Tyr Raman bands are not affected by the mutation. The Raman bands due to Trp residues other than Trp-182 seem not be affected, because derivative-like peaks that would reflect the shifts of these bands are not present in the difference spectrum. Accordingly, every Raman band in the difference spectrum is ascribed solely to Trp-182 of WT bR in the dark-adapted state. The conformation, hydrogen-bonding state, and environmental hydrophobicity of Trp-182 can be derived from the spectrum. Figure 3E shows the difference spectrum between the dark- and light-adapted states of WT bR. Any Trp Raman band of WT bR does not change on going from the dark-adapted state to the light-adapted state. Accordingly, the structural information to be obtained for the dark-adapted state may apply to the light-adapted state as well.

The frequency of Trp W3 mode is known to be sensitive to the absolute value of the torsion angle, $|\chi^{2,1}|$ about the bond (C_β−C_3) connecting the indole ring to the peptide mainchain. It varies from 1542 to 1557 cm^{-1} as a function of $|\chi^{2,1}|$ in a range 60−120° (*37*, *38*). The W3 frequency of Trp-182 (1550 cm^{-1}) corresponds to a $|\chi^{2,1}|$ angle of 93° with an estimated accuracy of ±6°. The full-width at half-maximum (FWHM) of the W3 band is 11 cm^{-1}, which is comparable to that of crystalline Trp (12 ± 1 cm^{-1}) (*39*). This narrow band width indicates that the conformation of the Trp-182 side chain is fixed at the $|\chi^{2,1}|$ angle mentioned above irrespective of the isomeric form of retinal (*all-trans* or 13-*cis*) in the dark-adapted state. The frequency of Trp W17 mode changes in the 883−871 cm^{-1} range with the strength of hydrogen bond at the indolyl nitrogen (*40*). For Trp-182, the W17 band is located in the middle (877 cm^{-1}) of the frequency range, indicating that the indole ring of Trp-182 is moderately hydrogen bonded to an acceptor. The W7 band of Trp usually splits into a doublet at 1360/1340 cm^{-1} due to Fermi resonance, and the intensity ratio of the doublet is known to be a marker of environmental hydrophobicity of the indole ring (*18*, *41*). The W7 band of Trp-182, however, shows up as a triplet with an additional peak at 1370 cm^{-1}. Such a triplet feature has been observed in the Raman spectra of neither Trp residues in proteins and peptides nor amino acid Trp in solids and solutions to our knowledge. The side chain of Trp-182 must be involved in an unusual interaction with the surroundings.

Figure 3C shows the result of the spectral subtraction, WT bR − W189F. As with Trp-182 (Figure 3B) the scattering from Tyr residues disappears in the difference spectrum, and

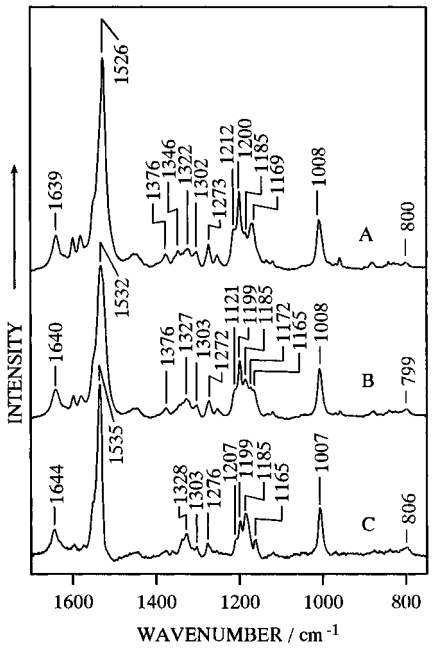

FIGURE 4: VISRR (514.5 nm) spectra of (A) WT bR, (B) W182F, and (C) the difference A − B in the light-adapted state. The bR or mutant was suspended in 5 mM HEPES buffer (pH 7.4) at a concentration of ~100 μM. A weak shoulder at 1551 cm^{-1} may be due to the L intermediate (*34*).

no derivative-like bands are seen. Thus, all Raman bands in the difference spectrum are attributable to Trp-189. The frequency and FWHM of the W3 band of Trp-189 are 1553 and 10 cm^{-1}, respectively, indicating that the side chain is fixed at a $|\chi^{2,1}|$ angle of 100° (±6°). The frequency of the W17 band (878 cm^{-1}) shows that the indolyl nitrogen of the Trp-189 side chain is moderately hydrogen bonded. The W7 intensity ratio for Trp-189 ($I_{1359}/I_{1337} = 0.9$) is much larger than that of Trp in aqueous solution ($I_{1361}/I_{1342} \approx 0.5$, Figure 3D), suggesting that Trp-189 is located in a hydrophobic environment. The hydrogen bonding and environmental hydrophobicity of Trp-189 are consistent with the intensity pattern of the Raman spectrum. The intensities of the W3, W7, W16, and W18 bands relative to the W1 and W2 bands are higher than that in aqueous Trp. According to an excitation profile study of the amino acid Trp (*42*), the W3, W7, W16, and W18 bands show large enhancement when the excitation wavelength is in resonance with the B_b transition (~215 nm), while the W1 and W2 bands are mainly enhanced by resonance with the higher lying B_a transition. Therefore, the high intensity of the W3, W7, W16, and W18 bands suggests a red shift (toward the Raman excitation wavelength 244 nm) of the B_b absorption of Trp-189. The red shift of the B_b absorption has been suggested from a 240 nm excited UVRR spectrum of WT bR (*20*). It is known that such a red shift is caused by hydrogen bonding of the indole ring in a hydrophobic environment (*36*).

Effects of Trp-182 Mutation on the Structure of Retinal. The absorption spectrum of the W182F mutant shows little change upon light adaptation, in contrast to significant changes in λ_{max} and intensity for WT bR and W189F (Figure 2A). This observation implies that the isomeric state of retinal in W182F might not be altered by the light adaptation. We examined the isomeric ratio of retinal in the light-adapted state by Raman spectroscopy using the excitation wavelength (514.5 nm) resonant with the retinal absorption. Figure 4 compares the visible resonance Raman (VISRR) spectra of WT bR and W182F. In the spectrum of WT bR (Figure 4A), the scattering from the *all-trans* retinal is dominant as expected, though traces of the 13-*cis* isomer are seen at 1185 and 800 cm^{-1} (*43*, *44*). The 1185 cm^{-1} band of 13-*cis* isomer, however, remains prominent for W182F (Figure 4B), in spite of the identical conditions of light adaptation. The spectral feature in the fingerprint (1400−1100 cm^{-1}) region is very close to that of dark-adapted WT bR (*44*), which contains a 6:4 mixture of 13-*cis* and *all-trans* isomers (*35*). From this spectrum, it appears that in light-adapted W182F nearly a half of retinal molecules are in the 13-*cis* configuration. A reconstitution study of bR with 13-desmethyl-retinal had shown that dark-adapted 13-desmethyl-bR contains predominantly the 13-*cis* isomer, and the retinal isomeric ratio does not change upon light adaptation (*45*). Stabilization of the 13-*cis* isomer has been reported also for 9-desmethyl-bR (*45*). This effect of methyl removal is analogous to that of the Trp-182→Phe mutation observed here. The lack of repulsion between Trp-182 and the methyl groups of retinal may facilitate the formation of the 13-*cis* isomer. In other words, a repulsion between Trp-182 and the methyl groups of retinal (see discussion below) may contribute to the destabilization of the 13-*cis* isomer in the retinal-binding pocket of bR.

The VISRR spectrum of the 13-*cis* isomer component in W182F has been obtained by subtracting the spectrum of WT bR from that of W182F (Figure 4C). The subtraction factor was selected to avoid a negative peak in the ethylenic stretch (1600−1500 cm^{-1}) region that would result from excessive subtraction. Although the spectral feature in the fingerprint region is similar to that of the 13-*cis* isomer of dark-adapted WT bR (*44*), the intensity of a band at 800 cm^{-1} is much weaker in W182F. The 800 cm^{-1} band has been assigned to the HOOP bend of C_{14}−H of retinal and the band borrows Raman intensity from the π conjugation system through a local twist near C_{14} (*44*). The weakness of the 800 cm^{-1} band indicates that the retinal chromophore becomes planar and relaxed upon substitution of the smaller Phe residue for Trp-182.

Effects of the Trp-182 mutation on the structure of 13-*cis* retinal appear in other frequency regions as well. The strong N−H bend mode of the PSB, which was observed at 1344 cm^{-1} for the 13-*cis* isomer of WT bR (*44*), is absent for W182F and the C=N stretch band of the PSB shifts from 1634 (WT bR; *44*) to 1644 cm^{-1} (W182F, Figure 4C). The absence of the N−H bend mode and the shift of the C=N stretch band have also been observed for the N intermediate of WT bR (*46*), in which the retinal chromophore takes the 13-*cis* configuration. The spectral similarity between the 13-*cis* isomer of W182F and the N intermediate of WT bR suggests that the retinal-binding pocket in W182F stabilizes an N-like structure of the retinal. According to a kinetic study of the photointermediates of W182F, the mutation results in stabilization of an N-like intermediate with a decay time of several seconds, which is 10^3-times longer than that of WT bR (*17*). Similar increase in the life time of the N intermediate has also been found for 9-desmethyl-bR (*17*, *47*). The prolonged life time of the N intermediate may be attributed to the lack of repulsion between Trp-182 and the 9-methyl group of retinal, as was pointed out previously (*17*). The mutation of Leu-93, which is in van der Waals contact with the 13-methyl group of retinal (*7*), to Ala also leads to

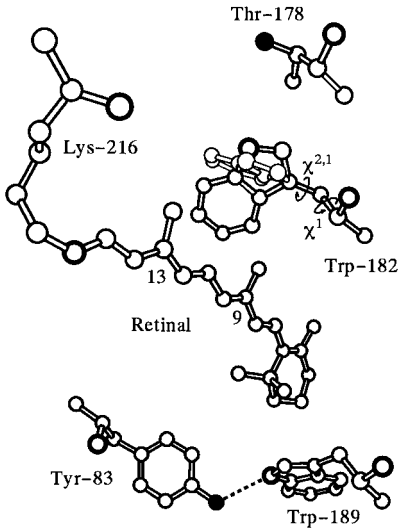

FIGURE 5: Arrangement of retinal, Trp-182 and Trp-189 in the retinal-binding pocket. The other residues constituting the binding pocket are omitted for clarity except for Tyr-83, Thr-178, and Lys-216. The atomic coordinates were taken from Brookhaven Protein Data Bank (*7*; identification code, 2BRD). For Trp-182, the $\chi^{2,1}$ angle is modified to 93°. The original conformation of Trp-182 is shown with thin lines. Circles with bold lines stand for nitrogen atoms and filled circles represent oxygen atoms. The broken line shows the hydrogen bond between Trp-189 and Tyr-83.

the stabilization of an intermediate that resembles the O (or N) intermediate of WT bR (*48*, *49*). It is likely that a tight packing of hydrophobic residues around the 9- and 13-methyl groups of retinal helps the retinal chromophore to reisomerize from 13-*cis* to *all-trans* in the transformation from the N to O intermediate.

DISCUSSION

In this study, we have demonstrated the utility of UVRR difference spectroscopy, combined with site-directed mutagenesis, in revealing the structure and interaction of specific Trp residues in bR. The 244 nm excited UVRR spectra of Trp-182 and Trp-189 were extracted from the spectrum of WT bR by using the mutants W182F and W189F. The difference spectra, with contributions from either single Trp residue only, provide information on the conformations, hydrogen-bonding states, and environmental hydrophobicity of Trp-182 and Trp-189. We will compare below the structural information obtained by UVRR spectroscopy with the molecular model obtained by electron diffraction (*6*, *7*).

Trp-189. The UVRR spectrum of Trp-189 shows that the residue has a $|\chi^{2,1}|$ angle of 100° and the indolyl nitrogen is moderately hydrogen bonded to a proton acceptor in a hydrophobic environment. In the electron diffraction model (*7*; Brookhaven Protein Data Bank identification code, 2BRD), the $\chi^{2,1}$ angle of Trp-189 is 98° and the indolyl nitrogen is hydrogen bonded to the hydroxyl oxygen of the Tyr-83 side chain with an N····O distance of 2.8 Å (Figure 5). The side chain conformation and hydrogen-bonding state of Trp-189 revealed by UVRR spectroscopy for the dark-adapted state are in agreement with those in the electron diffraction model for the light-adapted state. The environmental hydrophobicity of Trp-189 is also consistent with the model: Trp-189 side chain is surrounded by hydrophobic residues Ala-126, Trp-138, Leu-190, and Phe-208, and faces the β-ionone ring of retinal (*7*). It appears that the structure of bR around Trp-189 is not affected by the light-adaptation.

Trp-182. In contrast to Trp-189, there are discrepancies between the UVRR spectroscopy and the electron diffraction with respect to the conformation and hydrogen-bonding state of Trp-182. UVRR spectroscopy shows that the $|\chi^{2,1}|$ angle is 93° and the side chain is moderately hydrogen bonded to an acceptor. In the electron diffraction model, on the other hand, the $\chi^{2,1}$ is 33° and there are no proton acceptors within hydrogen-bonding distance from the indolyl nitrogen of Trp-182. One might attribute the discrepancies to structural differences between the dark- and light-adapted states. However, as described in the Results, the difference spectrum between the dark- and light-adapted states of WT bR shows no frequency shift for the conformation marker W3 and hydrogen-bonding marker W17 bands, suggesting that the isomerization of retinal between *all-trans* and 13-*cis* does not directly affect the bR structure in the vicinities of Trp residues. The discrepancies between the UVRR data and the electron diffraction model are not ascribed to the conformational difference of retinal between the dark- and light-adapted states.

According to a detailed examination of the crystal structure data of 61 globular proteins (*50*), the Trp residue in an α-helix is allowed to take only three conformations, which are represented by pairs of χ^1 (torsion angle around the $C_\alpha-C_\beta$ bond) and $\chi^{2,1}$. The possible conformations are $(\chi^1, \chi^{2,1}) = (-179°, -108°)$, (178°, 81°), and (−70°, 117°) with a standard deviation of about 10−20° for each angle. This conformational constraint arises from the steric repulsion between the Trp side chain and the peptide mainchain. Trp-189 in the electron diffraction model has χ^1 and $\chi^{2,1}$ angles that correspond to the first of the possible conformations. For Trp-182, the χ^1 angle in the electron diffraction model is −64°, which is close to the value in the third possible conformation. Since the $\chi^{2,1}$ angle is positive in the third possible conformation, the Raman finding, $|\chi^{2,1}| = 93°$, is reduced to $\chi^{2,1} = 93°$. The most probable conformation of Trp-182 may be represented by $(\chi^1, \chi^{2,1}) = (-64°, 93°)$.

To achieve the most probable conformation of Trp-182, we rotated the indole ring of Trp-182 about the $C_\beta-C_3$ bond from $\chi^{2,1} = 33°$ to 93° in the electron diffraction model (Figure 5). The conformational modification moves the indolyl nitrogen only little, and there are no proton acceptors within hydrogen-bonding distance. The closest proton acceptor is the OH group of Thr-178, but the distance between the indolyl nitrogen and the hydroxyl oxygen (4.1 Å) is too far to form a hydrogen bond. Small variations of the χ^1 and $\chi^{2,1}$ angles do not improve this situation. Accordingly, we conclude that Trp-182 is not hydrogen bonded with any amino acid residue. The electron diffraction study has pointed out the presence of a cavity near Trp-182 that is large enough to accommodate one water molecule (cavity VI) (*7*). The moderately hydrogen-bonded state of Trp-182 is accounted for only by assuming the presence of a water molecule in the cavity. It is probable that the water molecule in cavity VI bridges Trp-182 and Thr-178 by hydrogen bonding. Yamazaki et al. found a sharp indolyl N−H stretch band of Trp-182 at 3486 cm^{-1} in the FTIR difference spectrum of the L intermediate, and the band disappeared in the difference spectrum of the M intermediate of WT bR (*16*). This observation indicates that the indole ring of Trp-182 loses hydrogen bonding in the L intermediate

but is again hydrogen bonded in the M intermediate. The disruption and recovery of the hydrogen bond of Trp-182 may be caused by conformational change of the Trp side chain or a displacement of the water molecule, during the protein structural relaxation to accommodate the photochemically generated 13-*cis* isomeric form of the retinal.

The W7 band of Trp-182 exhibits an unusual triplet feature with an additional peak at 1370 cm^{-1} (Figure 3C). Generally, the splitting of the W7 band arises from Fermi resonance of the W7 fundamental with two combinations of out-of-plane vibrations, W25 (∼920 cm^{-1}) + W33 (∼420 cm^{-1}) and W28 (∼740 cm^{-1}) + W29 (∼610 cm^{-1}), and the W7 band is usually observed as a doublet with two peaks around 1360 and 1340 cm^{-1} (*18*, *19*, *41*). The additional peak at 1370 cm^{-1} may be assigned to one of the combinations, which is located in the 1360−1340-cm^{-1} region in the usual cases and shifted to 1370 cm^{-1} for Trp-182. The W29 mode involves the N−H and C−H HOOP vibrations of the five-membered ring of indole (*18*, *51*) and might be upshifted by hydrogen bonding at the N−H site. However, the W7 band of Trp-189 does not show a triplet feature, in spite of its hydrogen-bonding state similar to that of Trp-182. The W29 mode is unlikely to be the origin of the triplet. In contrast to W29, the W25 and W28 modes are HOOP vibrations of the six-membered ring of indole. In particular, the W28 mode is the in-phase HOOP vibration and is expected to be strong in infrared spectra (*51*). According to an FTIR study on WT bR and W182F, the W28 band of Trp-182 is located around 756 cm^{-1} (*14*, *17*), which is upshifted more than 10 cm^{-1} from that (∼742 cm^{-1}) of Trp-86 (*14*) and that (743−747 cm^{-1}) of acetyl tryptophan ethyl ester in solution (*41*). The high-frequency shift of the W28 mode may result in an upshift of the W28 + W29 combination, producing the additional peak at 1370 cm^{-1}. The six-membered ring of the Trp-182 side chain makes direct contact with the 9- and 13-methyl groups of retinal in the modified conformation (see Figure 5). This would be the basis of a coupling between the retinal polyene chain and the protein. The upshift of the W28 HOOP frequency and the triplet feature of the W7 band are thus attributed to the steric repulsion between Trp-182 and retinal.

The structure of retinal in W182F revealed by the present VISRR study (Figure 4) gives support for the repulsion between Trp-182 and retinal. As described in the Results, the population of the 13-*cis* isomer in light-adapted W182F is significantly higher than in WT bR, and the 13-*cis* isomer in W182F has a planar and relaxed structure in contrast to a twisted structure in WT bR. The stabilization of the relaxed 13-*cis* form of retinal in W182F can be ascribed to reduced retinal−protein repulsion associated with the replacement of Trp-182 by the smaller Phe residue. The benzene ring of the Phe side chain corresponds to the five-membered ring of the Trp side chain in spatial arrangement, and the six-membered ring of Trp-182, which would interact with the methyl groups of retinal, is absent in W182F. The lack of the repulsion between the six-membered ring of Trp-182 and the retinal methyl groups in W182F may result in a wider space for the retinal to isomerize to the bent 13-*cis* form and to take a relaxed planar structure.

In summary, the present study has demonstrated that the combination of UVRR difference spectroscopy and site-directed mutagenesis is a useful method to probe the structure of specific Trp residues in bR. The UVRR spectra of Trp-182 and Trp-189 have been extracted from the WT bR using the mutants W182F and W189F. From the UVRR spectra, the side chain conformation, $\chi^{2,1}$, and the hydrogen-bonding state at the indolyl nitrogen were derived for these Trp residues. The presence of a water molecule in cavity VI is suggested to account for the hydrogen-bonding state of Trp-182. The peculiar feature of the W7 band of Trp-182 is ascribed to a strong steric interaction between the side chain and the 9- and 13-methyl groups of retinal. This steric interaction is proposed to contribute to the destabilization of the 13-*cis* isomer in the retinal-binding pocket of bR.

REFERENCES

1. Rothschild, K. J. (1992) *J. Bioenerg. Biomembr. 24*, 147−167.
2. Oesterhelt, D., Tittor, J., and Bamberg, E. (1992) *J. Bioenerg. Biomembr. 24*, 181−191.
3. Krebs, M. P., and Khorana, H. G. (1993) *J. Bacteriol. 175*, 1555−1560.
4. Lanyi, J. K. (1993) *Biochim. Biophys. Acta 1183*, 241−261.
5. Maeda, A. (1995) *Isr. J. Chem. 35*, 387−400.
6. Henderson, R., Baldwin, J. M., Ceska, T. A., Zemlin, F., Beckmann, E., and Downing, K. H. (1990) *J. Mol. Biol. 213*, 899−929.
7. Grigorieff, N., Ceska, T. A., Downing, K. H., Baldwin, J. M., and Henderson, R. (1996) *J. Mol. Biol. 259*, 393−421.
8. Jang, D.-J., and El-Sayed, M. A. (1989) *Proc. Natl. Acad. Sci. U.S.A. 86*, 5815−5819.
9. Van den Berg, R., Jang, D.-J., and El-Sayed, M. A. (1990) *Biophys. J. 57*, 759−764.
10. Ahl, P. L., Stern, L. J., Düring, D., Mogi, T., Khorana, H. G., and Rothschild, K. J. (1988) *J. Biol. Chem. 263*, 13594−13601.
11. Mogi, T., Marti, T., and Khorana, H. G. (1989) *J. Biol. Chem. 264*, 14197−14201.
12. Wu, S., Jang, D.-J., El-Sayed, M. A., Marti, T., Mogi, T., and Khorana, H. G. (1991) *FEBS Lett. 284*, 9−14.
13. Roepe, P., Gray, D., Lugtenburg, J., van den Berg, E. M. M., Herzfeld, J., and Rothschild, K. J. (1988) *J. Am .Chem. Soc. 110*, 7223−7224.
14. Rothschild, K. J., Gray, D., Mogi, T., Marti, T., Braiman, M. S., Stern, L. J., and Khorana, H. G. (1989) *Biochemistry 28*, 7052−7059.
15. Maeda, A., Sasaki, J., Ohkita, Y. J., Simpson, M., and Herzfeld, J. (1992) *Biochemistry 31*, 12453−12455.
16. Yamazaki, Y., Sasaki, J., Hatanaka, M., Kandori, H., Maeda, A., Needleman, R., Shinada, T., Yoshihara, K., Brown, L. S., and Lanyi, J. K. (1995) *Biochemistry 34*, 577−582.
17. Weidlich, O., Schalt, B., Friedman, N., Sheves, M., Lanyi, J. K., Brown, L. S., and Siebert, F. (1996) *Biochemistry 35*, 10807−10814.
18. Harada, I., and Takeuchi, H. (1986) in *Spectroscopy of Biological Systems* (Clark, R. J. H., and Hester, R. E., Ed.) pp 113−175, John Wiley and Sons Ltd.
19. Austin, J. C., Jordan, T., and Spiro, T. G. (1993) in *Biomolecular Spectroscopy* (Clark, R. J. H., and Hester, R. E., Ed.) pp 55−127, John Wiley and Sons, Chichester.
20. Harada, I., Yamagishi, T., Uchida, K., and Takeuchi, H. (1990) *J. Am. Chem. Soc. 112*, 2443−2445.
21. Ames, J. B., Bolton, S. R., Netto, M. M., and Mathies, R. A. (1990) *J. Am. Chem. Soc. 112*, 9007−9009.
22. Netto, M. M., Fodor, S. P. A., and Mathies, R. A. (1990) *Photochem. Photobiol. 52*, 605−607.
23. Ames, J. B., Ros, M., Raap, J., Lugtenburg, J., and Mathies, R. A. (1992) *Biochemistry 31*, 5328−5334.
24. Harada, I., Yamagishi, T., Uchida, K., Hashimoto, S., Takeuchi, H., and Tokunaga, F. (1992) in *Time-Resolved Vibrational Spectroscopy* (Takahashi, H., Ed.) pp 49−52, Springer, Berlin.
25. Hashimoto, S., Miura, K., Yamagishi, T., Takeuchi, H., and Harada, I. (1992) *Photochem. Photobiol. 56*, 1097−1103.
26. Moënne-Loccoz, P., and Peticolas, W. L. (1992) *J. Am. Chem. Soc. 114*, 5893−5894.

27. Khorana, H. G., Gerber, G. E., Herlihy, W. C., Gray, C. P., Anderegg, R. J., Nihei, K., and Biemann, K. (1979) *Proc. Natl. Acad. Sci. U.S.A. 76*, 5046−5050.
28. Nie, B., Chang, M., Duschl, A., Lanyi, J. K., and Needleman, R. (1990) *Gene 90*, 169−172.
29. Needleman, R., Chang, M., Ni, B., Váró, G., Fornés, J., White, S. H., and Lanyi, J. K. (1991) *J. Biol. Chem. 266*, 11478−11484.
30. Oesterhelt, D., and Stoeckenius, W. (1974) *Methods Enzymol. 31*, 667−678.
31. Oesterhelt, D., Schuhmann, L., and Gruber, H. (1974) *FEBS Lett. 44*, 257−261.
32. Rehorek, M., and Heyn, M. P. (1979) *Biochemistry 18*, 4977−4983.
33. Hashimoto, S., Ikeda, T., Takeuchi, H., and Harada, I. (1993) *Appl. Spectrosc. 47*, 1283−1285.
34. Fodor, S. P. A., Pollard, W. T., Gebhard, R., van den Berg, E. M. M., Lugtenburg, J., and Mathies, R. A. (1988) *Proc. Natl. Acad. Sci. U.S.A. 85*, 2156−2160.
35. Song, L., Yang, D., El-Sayed, M. A., and Lanyi, J. K. (1955) *J. Phys. Chem. 99*, 10052−10055.
36. Chignell, D. A., and Gratzer, W. G. (1968) *J. Phys. Chem. 72*, 2934−2941.
37. Miura, T., Takeuchi, H., and Harada, I. (1989) *J. Raman Spectrosc. 20*, 667−671.
38. Maruyama, T., and Takeuchi, H. (1995) *J. Raman Spectrosc. 26*, 319−324.
39. Takeuchi, H., Nemoto, Y., and Harada, I. (1990) *Biochemistry 29*, 1572−1579.
40. Miura, T., Takeuchi, H., and Harada, I. (1988) *Biochemistry 27*, 88−94.
41. Harada, I., Miura, T., and Takeuchi, H. (1986) *Spectrochim. Acta 42A*, 307−312.
42. Su, C., Wang, Y., and Spiro, T. G. (1990) *J. Raman Spectrosc. 21*, 435−440.
43. Smith, S. O., Braiman, M. S., Myers, A. B., Pardoen, J. A., Courtin, J. M. L., Winkel, C., Lugtenburg, J., and Mathies, R. A. (1987) *J. Am. Chem. Soc. 109*, 3108−3125.
44. Smith, S. O., Pardoen, J. A., Lugtenburg, J., and Mathies, R. A. (1987) *J. Phys. Chem. 91*, 804−819.
45. Gärtner, W., Towner, P., Hopf, H., and Oesterhelt, D. (1983) *Biochemistry 22*, 2637−2644.
46. Fodor, S. P. A., Ames, J. B., Gebhard, R., van den Berg, E. M. M., Stoeckenius, W., Lugtenburg, J., and Mathies, R. A. (1988) *Biochemistry 27*, 7097−7101.
47. Weidlich, O., Friedman, N., Sheves, M., and Siebert, F. (1995) *Biochemistry 34*, 13502−13510.
48. Delaney, J. K., Schweiger, U., and Subramaniam, S. (1995) *Proc. Natl. Acad. Sci. U.S.A. 92*, 11120−11124.
49. Kandori, H., Yamazaki, Y., Hatanaka, M., Needleman, R., Brown, L. S., Richter, H.-T., Lanyi, J. K., and Maeda, A. (1997) *Biochemistry 36*, 5134−5141.
50. McGregor, M. J., Islam, S. A., and Sternberg, M. J. E. (1987) *J. Mol. Biol. 198*, 295−310.
51. Takeuchi, H., and Harada, I. (1986) *Spectrochim. Acta 42A*, 1069−1078.

BI971404F